

**NEUROMODELING OF MICROWAVE CIRCUITS EXPLOITING
SPACE MAPPING TECHNOLOGY**

J.W. Bandler, M.A. Ismail, J.E. Rayas-Sánchez and Q.J. Zhang

SOS-98-37-R

November 1998

© J.W. Bandler, M.A. Ismail, J.E. Rayas-Sánchez and Q.J. Zhang 1998

No part of this document may be copied, translated, transcribed or entered in any form into any machine without written permission. Address inquiries in this regard to Dr. J.W. Bandler. Excerpts may be quoted for scholarly purposes with full acknowledgment of source. This document may not be lent or circulated without this title page and its original cover.

NEUROMODELING OF MICROWAVE CIRCUITS EXPLOITING SPACE MAPPING TECHNOLOGY

J.W. Bandler, M.A. Ismail, J.E. Rayas-Sánchez and Q.J. Zhang

Simulation Optimization Systems Research Laboratory
and Department of Electrical and Computer Engineering
McMaster University, Hamilton, Canada L8S 4K1

Tel 905 628 9671
Fax 905 628 1578
Email j.bandler@ieee.org

Abstract

For the first time, we present neuromodeling of microwave circuits based on Space Mapping (SM) technology. SM based neuromodels decrease the cost of training, improve generalization ability and reduce the complexity of the ANN topology w.r.t. classical neuromodeling. Three novel techniques are proposed to generate SM based neuromodels: Space-Mapped Neuromodeling (SMN), Frequency-Dependent Space-Mapped Neuromodeling (FDSMN), and Frequency Space-Mapped Neuromodeling (FSMN). Huber optimization is proposed to train the neuro-space-mapping (NSM). The techniques are illustrated by a microstrip right angle bend and a microstrip line with high dielectric constant.

SUMMARY

Introduction

A powerful new concept in neuromodeling of microwave circuits based on Space Mapping technology is presented. The ability of Artificial Neural Networks (ANN) to model high-dimensional and highly nonlinear problems is exploited in the implementation of the Space Mapping concept. By taking

This work was supported in part by the Natural Sciences and Engineering Research Council of Canada under Grants OGP0007239 and STP0201832, and through the Micronet Network of Centres of Excellence. J.E. Rayas-Sánchez is funded by CONACYT (Consejo Nacional de Ciencia y Tecnología, Mexico), as well as by ITESO (Instituto Tecnológico y de Estudios Superiores de Occidente, Mexico).

J.W. Bandler is also with Bandler Corporation, P.O. Box 8083, Dundas, Ontario, Canada L9H 5E7.

Q.J. Zhang is with the Department of Electronics, Carleton University, 1125 Colonel By Drive, Ottawa, Canada K1S 5B6.

advantage of the vast set of empirical models already available, Space Mapping based neuromodels decrease the number of EM simulations for training, improve generalization ability and reduce the complexity of the ANN topology with respect to the classical neuromodeling approach.

Three innovative techniques are proposed to create Space Mapping based neuromodels for microwave circuits: Space-Mapped Neuromodeling (SMN), Frequency-Dependent Space-Mapped Neuromodeling (FDSMN) and Frequency Space-Mapped Neuromodeling (FSMN). In both the FDSMN and FSMN approaches, a frequency-sensitive neuromapping is established to expand the frequency region of accuracy of the empirical models already available for microwave components that were developed using quasi-static analysis.

For the first time, Huber optimization is proposed to efficiently train the neuro-space-mapping (NSM), as a powerful alternative to the popular backpropagation algorithm. The Space Mapping based neuromodeling techniques are illustrated by two case studies: a microstrip right angle bend and a microstrip line with high dielectric constant. We contrast our approach with the classical neuromodeling approach as well as with other state-of-the-art neuromodeling techniques.

Space Mapping Concept

Space Mapping (SM) is a novel concept for circuit design and optimization that combines the computational efficiency of coarse models with the accuracy of fine models. The coarse models are typically empirical equivalent circuit engineering models, which are computationally very efficient but often have a limited validity range for their parameters, beyond which the simulation results may become inaccurate. On the other hand, detailed or “fine” models can be provided by an electromagnetic (EM) simulator, or even by direct measurements: they are very accurate but CPU intensive. The SM technique establishes a mathematical link between the coarse and the fine models, and directs the bulk of CPU intensive evaluations to the coarse model, while preserving the accuracy and confidence offered by the fine model. The SM technique was originally developed by Bandler *et al.* [1].

Let the vectors \mathbf{x}_c and \mathbf{x}_f represent the design parameters of the coarse and fine models,

respectively, and $\mathbf{R}_c(\mathbf{x}_c)$ and $\mathbf{R}_f(\mathbf{x}_f)$ the corresponding model responses. \mathbf{R}_c is much faster to calculate but less accurate than \mathbf{R}_f .

As illustrated in Fig. 1, the aim of SM optimization is to find an appropriate mapping \mathbf{P} from the fine model parameter space \mathbf{x}_f to the coarse model parameter space \mathbf{x}_c

$$\mathbf{x}_c = \mathbf{P}(\mathbf{x}_f) \quad (1)$$

such that

$$\mathbf{R}_c(\mathbf{P}(\mathbf{x}_f)) \approx \mathbf{R}_f(\mathbf{x}_f) \quad (2)$$

Once the mapping is found, the coarse model can be used for fast and accurate simulations.

Neuromodeling Microwave Circuits

The ability to learn and generalize from data, the non-linear processing nature, and the massively parallel structure make the ANN particularly suitable in modeling high-dimensional and highly nonlinear problems, as in the case of microwave circuits.

The size of an ANN model does not grow exponentially with dimension and, in theory, can approximate any degree of nonlinearity to any desired level of accuracy, provided a deterministic relationship between input and target exists [2]. The most widely used ANN paradigm in the microwave arena is the multi-layer perceptron (MLP), which is usually trained by the well established backpropagation algorithm.

ANN models are computationally more efficient than EM or physics-based models and can be more accurate than empirical models. It has been demonstrated [3, 4] that ANNs are suitable models for microwave circuit yield optimization and statistical design.

For microwave problems the learning data is usually obtained by either EM simulation or by measurement. This is very expensive since the simulation/measurements must be performed for many combinations of different values of geometrical, material, process and input signal parameters. This is the principal drawback of classical ANN modeling. Without sufficient learning samples, the neural

models may not be very reliable.

Innovative strategies have been proposed to reduce the learning data needed and to improve the generalization capabilities of an ANN by incorporating empirical models. In the knowledge based ANN approach [5] (KBNN), a non fully connected network is used, with a layer assigned to the microwave knowledge in the form of single or multidimensional functions. In the hybrid EM-ANN modeling approach [6], the difference in S -parameters between the available coarse model and the fine model is used to train the corresponding ANN, reducing the number of fine model simulations due to a simpler input-output relationship.

Space-Mapped Neuromodeling

In the Space-Mapped Neuromodeling (SMN) approach the mapping from the fine to the coarse parameter space is implemented by an ANN. It can be found by solving the optimization problem

$$\min_N \left\| [\mathbf{e}_1^T \quad \mathbf{e}_2^T \quad \cdots \quad \mathbf{e}_l^T]^T \right\| \quad (3)$$

where N contains the internal parameters of the neural network (weights, bias, etc.) selected as optimization variables, l is the total number of learning samples, and \mathbf{e}_j is the error vector given by

$$\mathbf{e}_j = \mathbf{R}_f(\mathbf{x}_{f_j}) - \mathbf{R}_c(\mathbf{x}_{f_j}, \mathbf{N}), \quad j = 1, 2, \dots, l \quad (4)$$

In other words, we have to find the optimal set of the internal parameters of the ANN, N^* , such that the coarse model response is as close as possible to the fine model response for all the learning points.

Fig. 2(a) illustrates the SMN concept. Once the mapping is found, i.e., once the ANN is trained, a space-mapped neuromodel (Fig. 2(b)) for fast, accurate evaluations is immediately available.

Including Frequency in the Neuromapping

Many available empirical models are based on quasi-static analysis: they usually yield good accuracy over a limited lower range of frequencies. We overcome this limitation through a frequency-sensitive mapping from the fine to the coarse parameter space. This is realized by considering frequency as an extra input variable of the ANN that implements the mapping. We propose Frequency Dependent

Space Mapped Neuromodeling (FDSMN) and Frequency Space Mapped Neuromodeling (FSMN).

As illustrated in Fig. 3, in the FDSMN approach both coarse and fine models are simulated at the same frequency, but the mapping from the coarse to the fine parameter space is dependent on the frequency. With a more comprehensive domain, the FSMN technique establishes a mapping not only for the design parameters but also for the frequency variable, such that the coarse model is simulated at a mapped frequency f_c to match the fine model response. This is realized by adding an extra output to the ANN that implements the mapping, as shown in Fig. 4.

Starting Point and Learning Data Samples

The starting point for the optimization problem stated in (3) is the initial set of internal parameters of the ANN, $\mathbf{N}^{(1)}$, that will be chosen assuming that the coarse model is actually a good model and therefore the mapping is not necessary. In other words, $\mathbf{N}^{(1)}$ is chosen such that $\mathbf{x}_{c_j} \approx \mathbf{x}_{f_j}$ for $j = 1, 2, \dots, t$, where t is the total number of test points. This is applicable to both FDSMN and FSMN approaches ($f_{c_j} \approx freq_j$ for FSMN).

The ANN must be trained to learn the mapping between the coarse and the fine parameter spaces within the region of interest. In order to keep a reduced set of learning data samples, an n -dimensional star distribution for the base learning points is considered in this work, as in [7] (see Fig. 5). It is evident that the number of base points for a NSM with n inputs is $B_p = 2n + 1$, hence the number of learning samples is $l = B_p F_p$, where F_p is the total number of frequency points per frequency sweep.

Since we want to maintain a minimum number of learning points (or fine evaluations), the complexity of the NSM (the number of hidden neurons) is critical. If the complexity is too large, the training error is very small but the generalization ability is deteriorated. We have to find the simplest ANN that gives adequate training error and acceptable generalization performance.

Mapping with a Three Layer Perceptron

A possible scheme to implement the mapping using a three-layer perceptron with k hidden

neurons, for both the SMN approach as well as the FDSMN approach, is illustrated in Fig. 6. Here, the total number of optimization variables for (3) is $2k(n+1)+n$, where n is the number of physical parameters to be mapped and k is the number of hidden neurons. The adaptation of this paradigm to the case of FSMN is similar, by considering an additional output for the mapped frequency f_c .

The SMN approach can be considered and implemented as a special case of the FDSMN approach, by making $v_{n+1}=0$ in the three-layer perceptron (see Fig. 6). In other words, the optimal response of the FDSMN with $v_{n+1}=0$ is equivalent to the optimal response of the corresponding SMN.

Case Study 1: A Microstrip Right Angle Bend

Consider a microstrip right angle bend, as illustrated in Fig. 7, with the following input parameters: conductor width W , substrate height H , substrate dielectric constant ϵ_r , and operating frequency $freq$. Several neuromodels exploiting SM technology are developed for the region of interest shown in Table I.

Gupta's model [8], consisting of a lumped LC circuit whose parameter values are given by analytical functions of the physical quantities W , H and ϵ_r , is taken as the "coarse" model and implemented in *OSA90/hope*TM [9]. Sonnet's *em*TM [10] is used as the fine model. To parameterize the structure, the Geometry Capture [11] technique available in *Empipe*TM [12] is utilized.

Fig. 8 shows typical responses of the coarse and fine models before any neuromodeling, using a frequency step of 2 GHz ($F_p = 21$). The coarse and fine models are compared in Fig. 9 using 50 random test points with uniform statistical distribution within the region of interest ($t = 1050$). Gupta's model, in this region of physical parameters, yields acceptable results for frequencies less than 10 GHz.

With a star distribution for the learning base points ($B_p = 7$), 147 learning samples ($l = 147$) are used for the three SM neuromodels, and the corresponding ANNs were implemented and trained within *OSA90*. Huber optimization was employed as the training algorithm, exploiting its robust characteristics for data fitting [13].

Fig. 10 shows the results for the SMN model implemented with a three layer perceptron with 3 input neurons, 6 hidden neurons, and 3 output neurons (3LP:3-6-3). A FDSMN model is developed using a 3LP:4-7-3, and the improved results are shown in Fig. 11. In Fig. 12 the results for the FSMN model with a 3LP:4-8-4 are shown, that are even better (as expected). To implement the FSMN approach, an *OSA90* child program is employed to simulate the coarse model with a different frequency variable using Datapipe. It is seen that the FSMN model yields excellent results for the whole frequency range of interest, overcoming the frequency limitations of the empirical model by a factor of four.

To compare these results with those from a classical neuromodeling approach, an ANN was developed using *NeuroModeler* [14]. Training the ANN with the same 147 learning samples, the best results were obtained for a 3LP:4-15-4 trained with the conjugate gradient and quasi-Newton methods. Due to the small number of learning samples, this approach did not provide good generalization capabilities, as illustrated in Fig. 13. To produce similar results to those in Fig. 12 using the same ANN complexity, the learning samples have to increase from 147 to 315.

Fig. 14 summarizes the different neuromodeling approaches applied to this case study.

Case Study 2: Microstrip Line with High Dielectric Constant

Fig. 15 illustrates a microstrip line to be modeled in the region of interest shown in Table II. This structure is a typical subsection of a high-temperature superconducting (HTS) quarter-wave parallel coupled-line microstrip filter.

The Kirschning and Jansen model of a microstrip line is taken as the “coarse” model. This model is accurate for the range of parameters [9]

$$0.1 \leq \frac{W}{H} \leq 10 \quad (5a)$$

$$1 \leq \epsilon_r \leq 18 \quad (5b)$$

$$freq (GHz) \leq \frac{30}{H (mm)} \quad (5c)$$

It is implemented using the built-in linear elements MSL (microstrip line) and MSUB (microstrip

substrate definition) available in *OSA90*. Sonnet's *em* driven by *Empipe* was employed as the fine model.

The coarse and fine models before neuromodeling are compared in Fig. 16, showing that Jansen model exhibits errors in the reflection coefficient due to the high dielectric constant, especially in the phase of S_{11} (the errors in S_{21} are negligible). A frequency step of 0.05 GHz ($F_p = 8$) and 100 random test points with uniform statistical distribution were used (800 test samples). From (5c), it is seen that the coarse model is being used in a relatively low frequency range, hence the NSM does not need to be frequency-sensitive in this case.

With a star distribution for the learning base points ($B_p = 9$), a total of 72 learning samples ($l = 72$) are used. A SMN is implemented and trained within *OSA90/hope*, using Huber optimization. Here, a simple 3LP:4-4-4 is sufficient, which reflects the small nonlinearity needed in the mapping. Substantial improvements are obtained, as shown in Fig. 17.

Relationship between SM Based Neuromodeling and GSM Modeling

A Generalized Space Mapping approach to device modeling is presented in [15], in which a comprehensive tableau for a linear mapping applicable for both the design parameters as well as the frequency variable is formulated. Our SM based neuromodeling approach is capable of establishing a nonlinear mapping for both the design parameters (SMN modeling) and the frequency (FDSMN and FSMN). Due to the nonlinear nature of the neuromapping, the SM based neuromodeling techniques do not require the frequency range to be segmented in case of severe misalignment between the coarse and fine frequency responses, in contrast with the piecewise linear approach needed for the GSM techniques. Furthermore, in the FSMN technique, a coupling between the transformed frequency f_c and the design parameters \mathbf{x}_f is in principle assumed, which represents the most general case in the GSM approach.

Conclusions

We present novel applications of Space Mapping technology to the neuromodeling of microwave circuits. Three powerful techniques to generate SM based neuromodels are described and illustrated: Space-Mapped Neuromodeling (SMN), Frequency-Dependent Space-Mapped Neuromodeling (FDSMN)

and Frequency Space-Mapped Neuromodeling (FSMN). These techniques exploit the vast set of empirical models already available, decrease the number of fine model evaluations needed for training, improve generalization ability and reduce the complexity of the ANN topology w.r.t. the classical neuromodeling approach. Frequency-sensitive neuromapping (FDSMN and FSMN) is demonstrated to be a clever strategy to expand the usefulness of empirical models that were developed using quasi-static analysis. As an original alternative to the classical backpropagation algorithm, Huber optimization is employed to efficiently train the neuromapping, exploiting its robust characteristics for data fitting.

References

- [1] J.W. Bandler, R.M. Biernacki, S.H. Chen, P.A. Grobelny and R.H. Hemmers, "Space mapping technique for electromagnetic optimization," *IEEE Trans. Microwave Theory Tech.*, vol. 42, 1994, pp. 2536-2544.
- [2] H. White, A.R. Gallant, K. Hornik, M. Stinchcombe and J. Wooldrige, *Artificial Neural Networks: Approximation and Learning Theory*. Oxford, UK: Blackwell, 1992.
- [3] A.H. Zaabab, Q.J. Zhang and M.S. Nakhla, "A neural network modeling approach to circuit optimization and statistical design," *IEEE Trans. Microwave Theory Tech.*, vol. 43, 1995, pp. 1349-1358.
- [4] P. Burrascano, M. Dionigi, C. Fancelli and M. Mongiardo, "A neural network model for CAD and optimization of microwave filters," *IEEE MTT-S Int. Microwave Symp. Dig.* (Baltimore, MD), 1998, pp. 13-16.
- [5] F. Wang and Q.J. Zhang, "Knowledge based neuromodels for microwave design," *IEEE Trans. Microwave Theory Tech.*, vol. 45, 1997, pp. 2333-2343.
- [6] P. Watson and K.C. Gupta, "EM-ANN models for microstrip vias and interconnects in multilayer circuits," *IEEE Trans. Microwave Theory Tech.*, vol. 44, 1996, pp. 2495-2503.
- [7] R.M. Biernacki, J.W. Bandler, J. Song and Q.J. Zhang, "Efficient quadratic approximation for statistical design," *IEEE Trans. Circuit Syst.*, vol. 36, 1989, pp. 1449-1454.
- [8] K.C. Gupta, R. Garg and I.J. Bahl, *Microstrip Lines and Slotlines*. Dedham, MA: Artech House, 1979.
- [9] *OSA90/hope*TM Version 4.0, formerly Optimization Systems Associates Inc., P.O. Box 8083, Dundas, Ontario, Canada L9H 5E7, now HP EEsof Division, Hewlett-Packard Company, 1400 Fountaingrove, Parkway, Santa Rosa, CA 95403-1799.
- [10] *em*TM Version 4.0b, Sonnet Software, Inc., 135 Old Cove Road, Suite 203, Liverpool, NY 13090-3774, 1997.

- [11] J.W. Bandler, R.M. Biernacki and S.H. Chen, "Parameterization of arbitrary geometrical structures for automated electromagnetic optimization," *IEEE MTT-S Int. Microwave Symp. Dig.* (San Francisco, CA), 1996, pp. 1059-1062.
- [12] *Empipe*TM Version 4.0, formerly Optimization Systems Associates Inc., P.O. Box 8083, Dundas, Ontario, Canada L9H 5E7, now HP EEsof Division, Hewlett-Packard Company, 1400 Fountaingrove, Parkway, Santa Rosa, CA 95403-1799.
- [13] J.W. Bandler, S.H. Chen, R.M. Biernacki, L. Gao, K. Madsen and H. Yu, "Huber optimization of circuits: a robust approach," *IEEE Trans. Microwave Theory Tech.*, vol. 41, 1993, pp. 2279-2287.
- [14] *NeuroModeler*, Prof. Q.J. Zhang, Dept. of Electronics, Carleton University, 1125 Colonel By Drive, Ottawa, Ontario, Canada, K1S 5B6.
- [15] J.W. Bandler, N. Georgieva, M.A. Ismail, J.E. Rayas-Sánchez and Q.J. Zhang, "A generalized space mapping tableau approach to device modeling," *IEEE MTT-S Int. Microwave Symp.* (Anaheim, CA), 1999, submitted.

TABLE I
REGION OF INTEREST FOR THE
MICROSTRIP RIGHT ANGLE BEND

Parameter	Minimum value	Maximum value
W	20 mil	30 mil
H	8 mil	16 mil
ϵ_r	8	10
$freq$	1 GHz	41 GHz

TABLE II
REGION OF INTEREST FOR THE MICROSTRIP LINE

Parameter	Minimum value	Maximum value
W	5 mil	9 mil
H	15 mil	25 mil
ϵ_r	20	25
L	40 mil	60 mil
$freq$	3.7 GHz	4.1 GHz

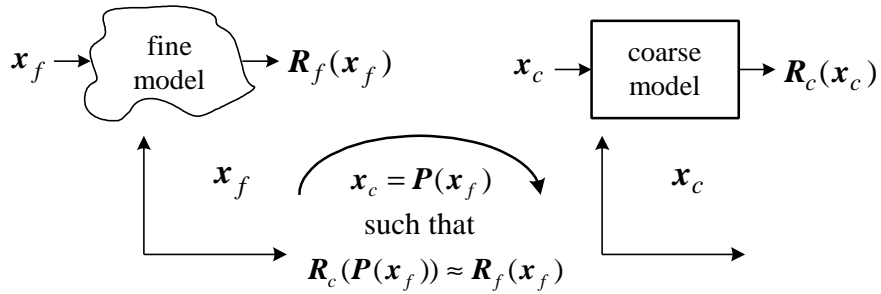


Fig. 1. Illustration of the aim of Space Mapping.

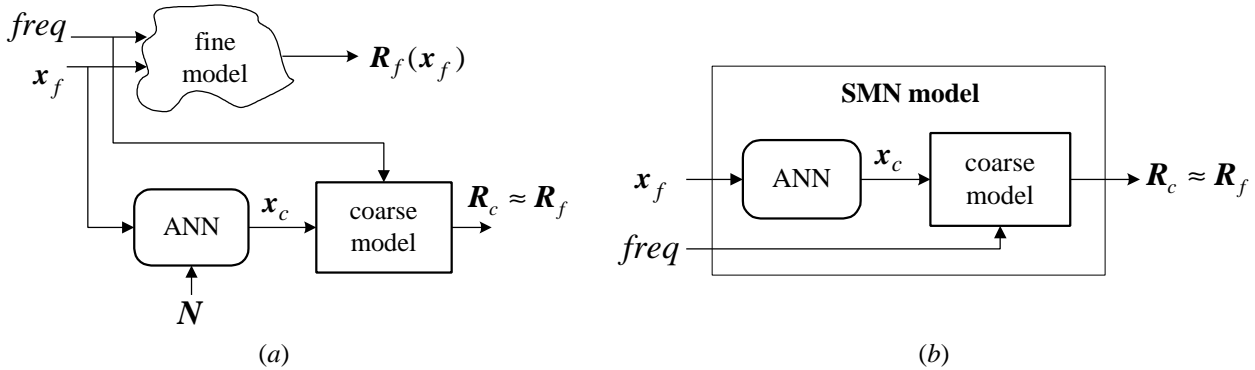


Fig. 2. Space Mapped Neuromodeling concept: (a) SM neuromodeling, (b) SMN model.

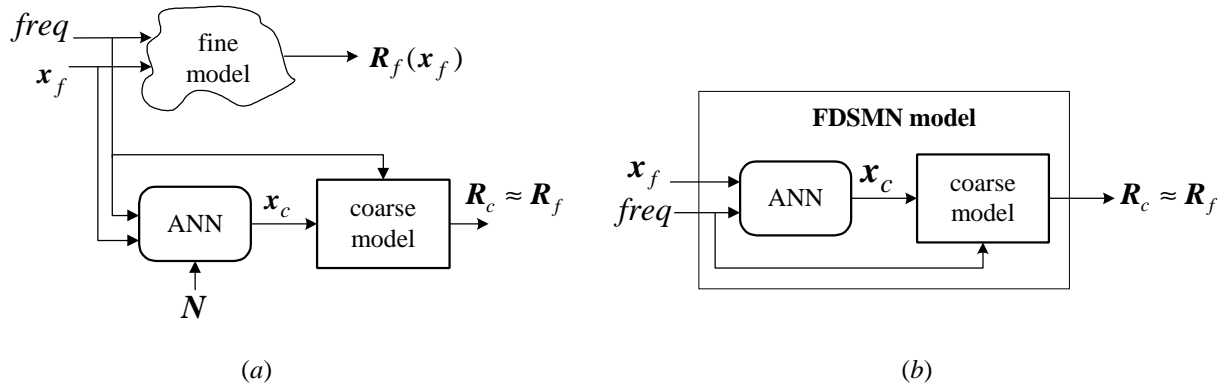


Fig. 3. Frequency Dependent Space Mapped Neuromodeling concept: (a) FDSM neuromodeling, (b) FDSMN model.

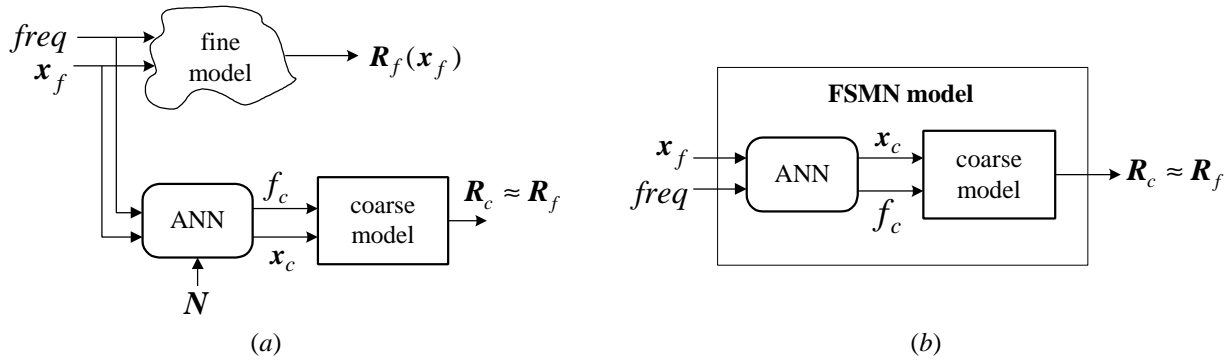


Fig. 4. Frequency Space Mapping Neuromodeling concept: (a) FSM neuromodeling, (b) FSMN model.

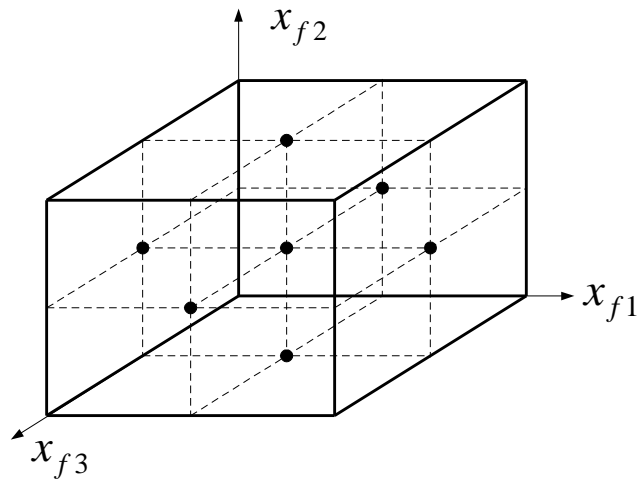


Fig. 5. Three-dimensional star distribution for the learning base points.

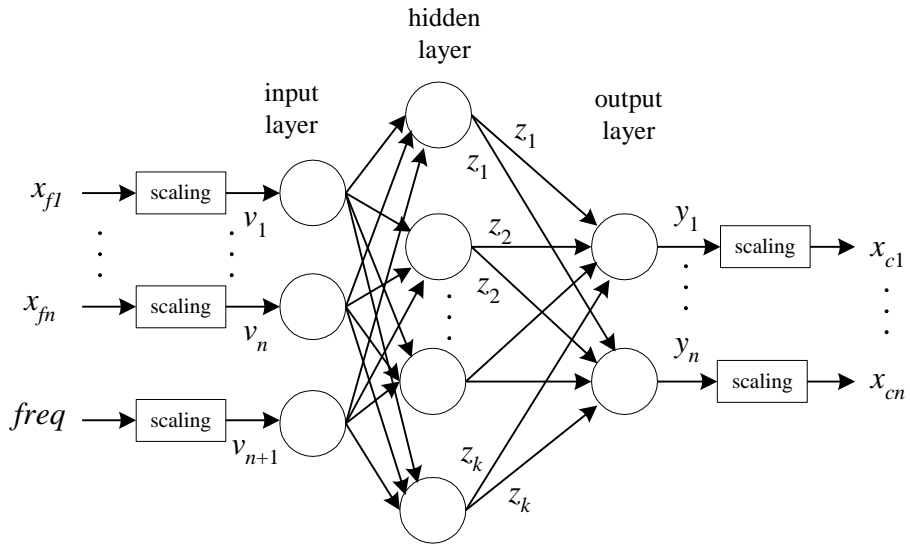


Fig. 6. Implementing the frequency-dependent neuromapping with a three layer perceptron.

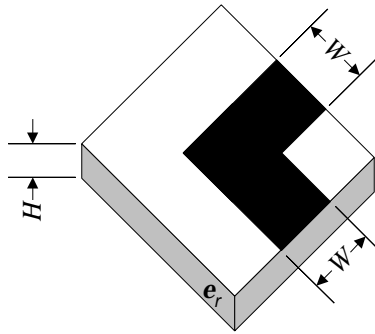


Fig. 7. Microstrip right angle bend.

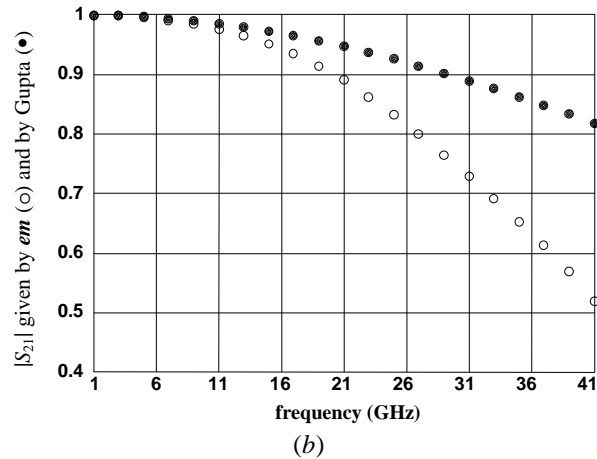
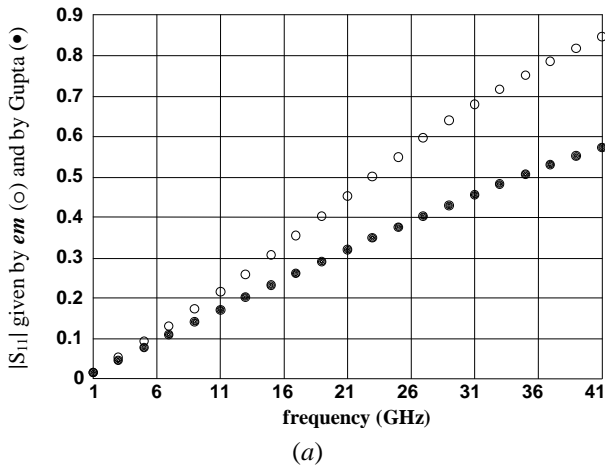


Fig. 8. Typical responses of the right angle bend using *em* (o) and Gupta model (•) before any neuromodeling: (a) $|S_{11}|$, (b) $|S_{21}|$.

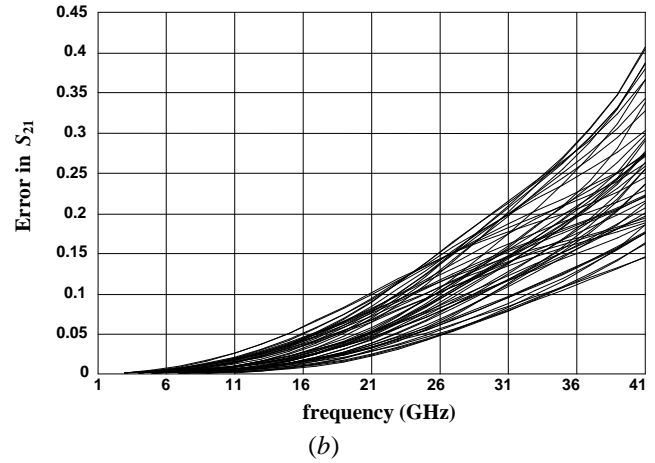
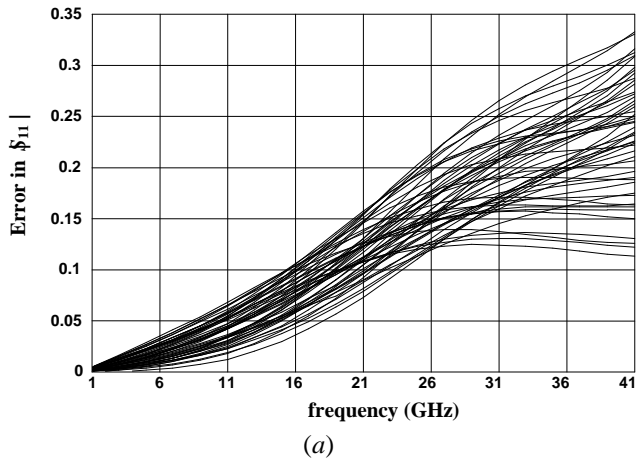


Fig. 9. Comparison between *em* and Gupta model of a right angle bend:
 (a) error in $|S_{11}|$ with respect to *em*, (b) error in $|S_{21}|$ with respect to *em*.

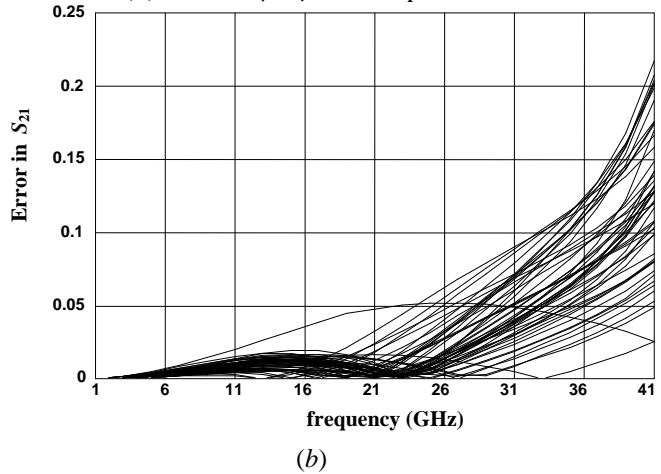
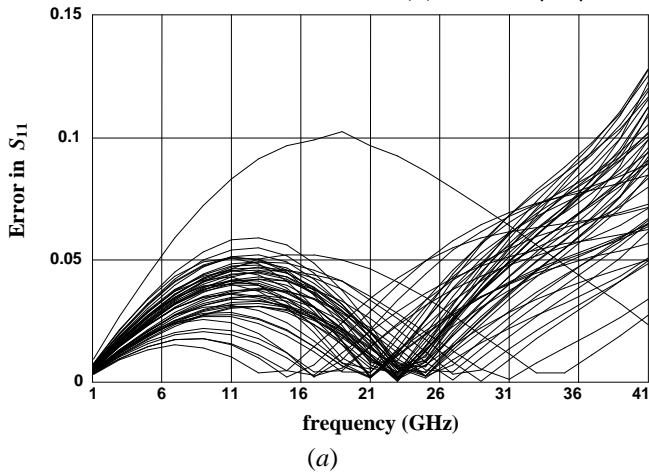


Fig. 10. Comparison between *em* and SMN model of a right angle bend:
 (a) error in $|S_{11}|$ with respect to *em*, (b) error in $|S_{21}|$ with respect to *em*.

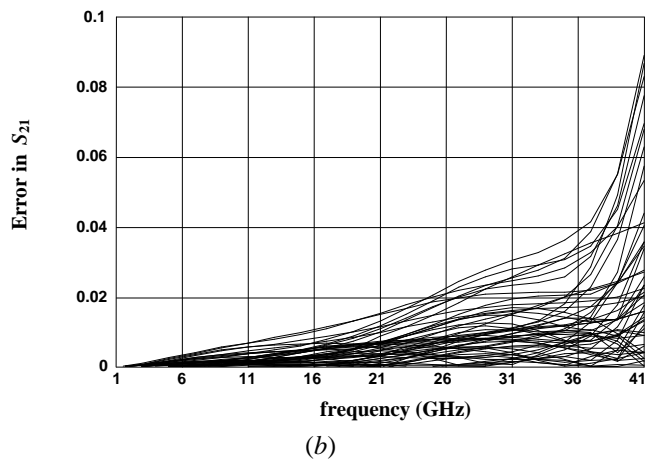
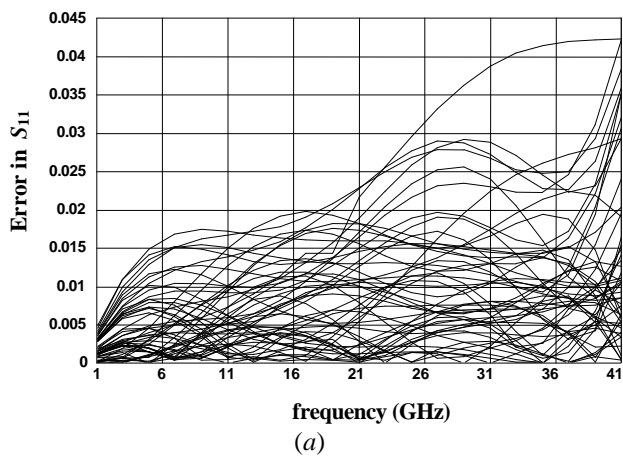
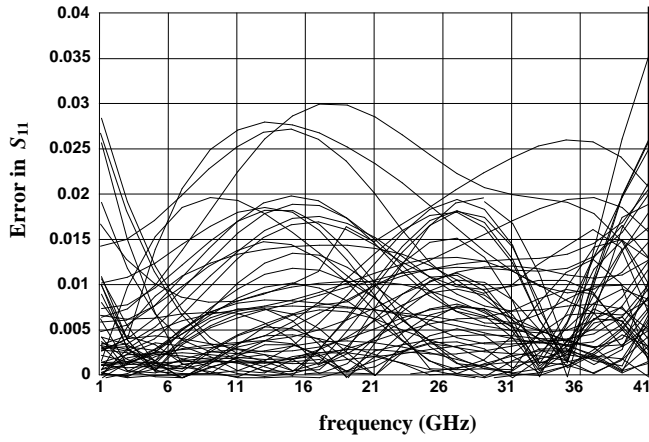
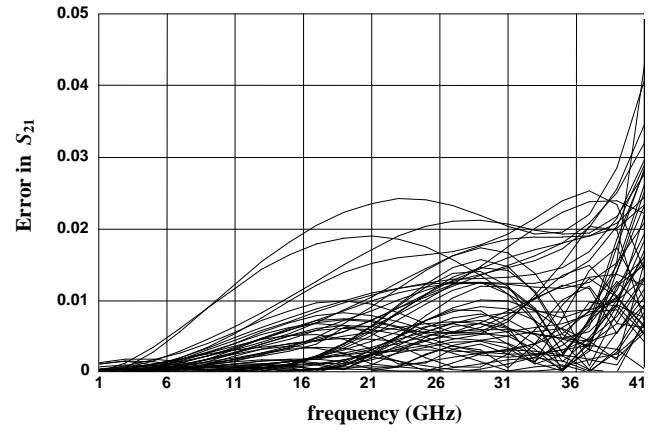


Fig. 11. Comparison between *em* and FDSMN model of a right angle bend:
 (a) error in $|S_{11}|$ with respect to *em*, (b) error in $|S_{21}|$ with respect to *em*.

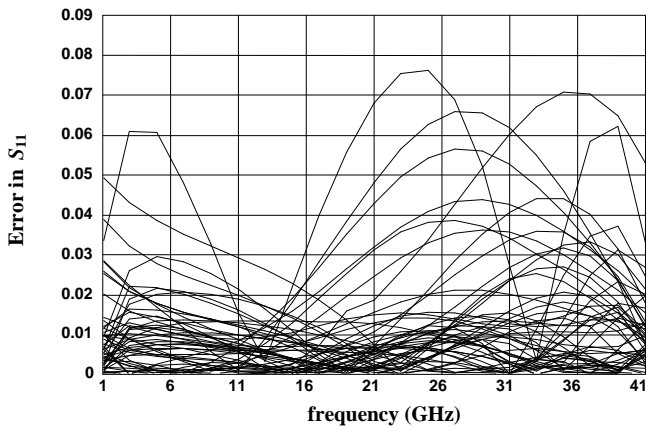


(a)

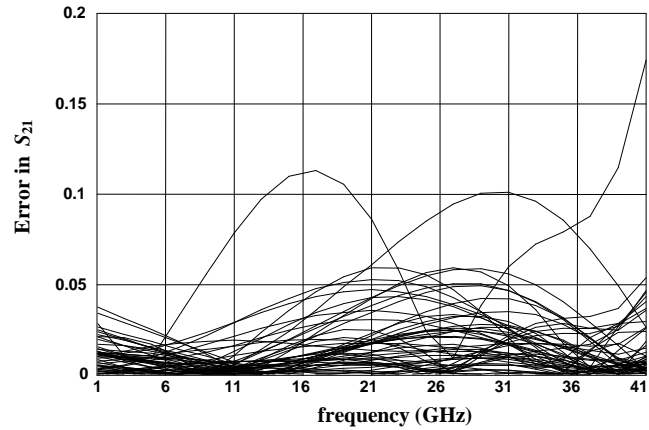


(b)

Fig. 12. Comparison between *em* and FSMN model of a right angle bend:
 (a) error in $|S_{11}|$ with respect to *em*, (b) error in $|S_{21}|$ with respect to *em*.



(a)



(b)

Fig. 13. Comparison between *em* and classical neuromodel of a right angle bend:
 (a) error in $|S_{11}|$ with respect to *em*, (b) error in $|S_{21}|$ with respect to *em*.

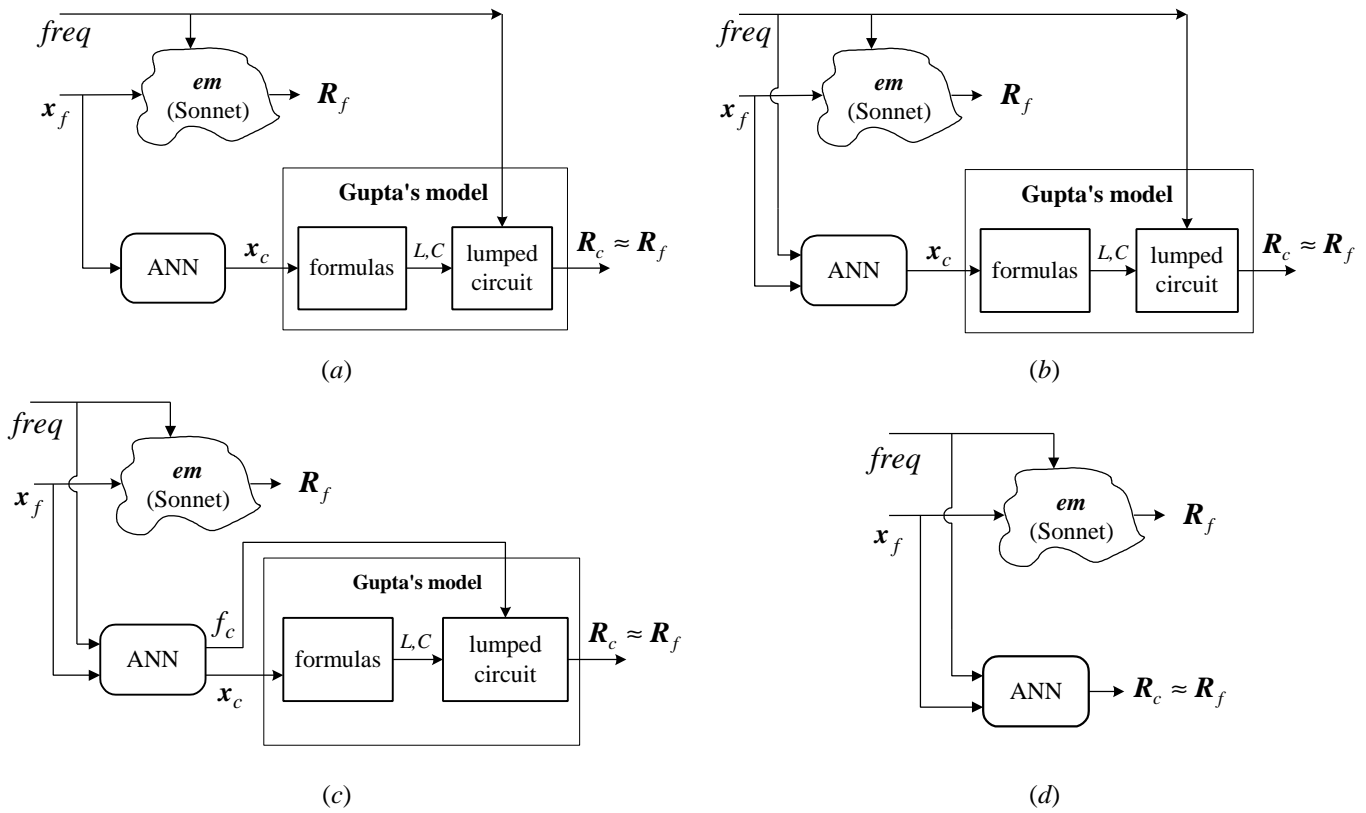


Fig. 14. Different neuromodeling approaches for the right angle bend: (a) SMN, (b) FDSMN, (c) FSMN, and (d) classical neuromodeling.

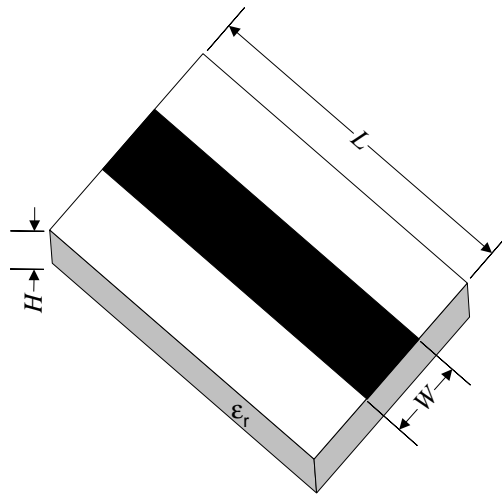
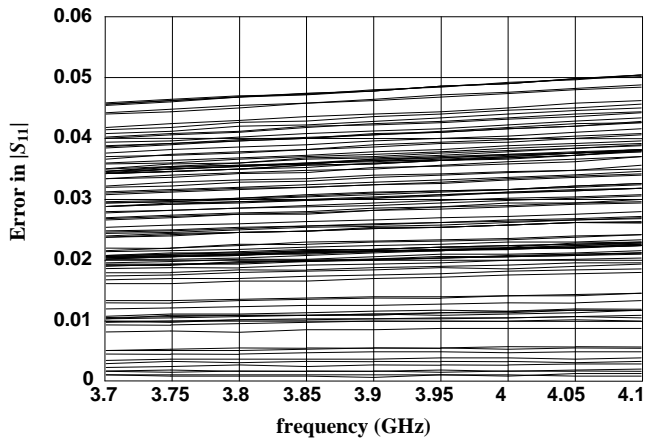
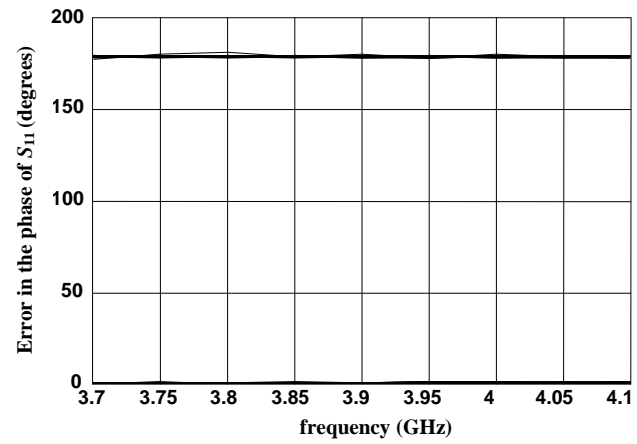


Fig. 15. Microstrip line with high dielectric constant.

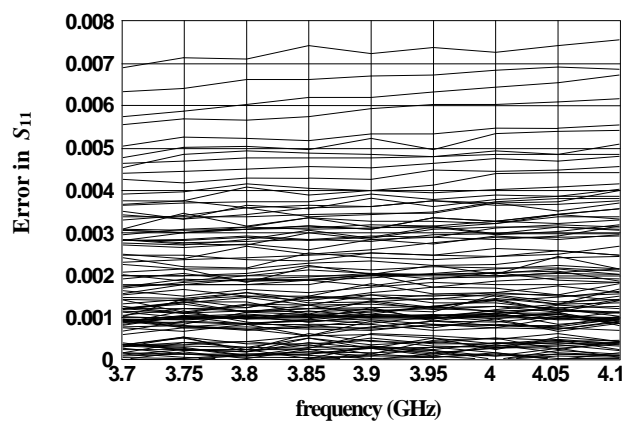


(a)

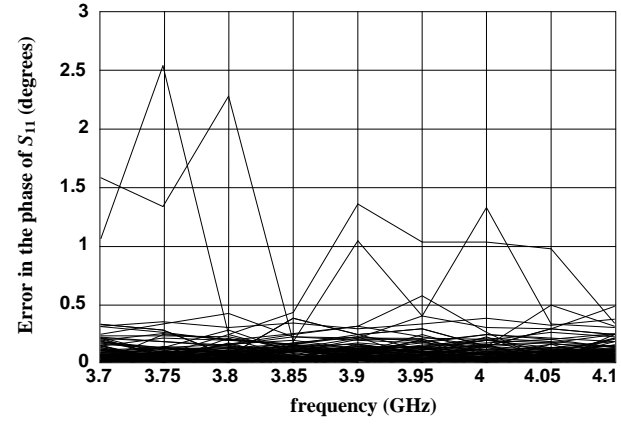


(b)

Fig. 16. Comparison between *em* and Jansen model of a microstrip line: (a) error in $|S_{11}|$ with respect to *em*, (b) error in the phase of S_{11} with respect to *em*.



(a)



(b)

Fig. 17. Comparison between *em* and SMN model of a microstrip line: (a) error in $|S_{11}|$ with respect to *em*, (b) error in the phase of S_{11} with respect to *em*.